Dynamically tuned interferometers for the observation of gravitational waves from coalescing compact binaries

Brian J. Meers*
Department of Physics and Astronomy, University of Glasgow, Glasgow G12 8QQ, Scotland

Andrzej Krolak
Institute of Mathematics, Polish Academy of Sciences, Warsaw, Poland

J. Alberto Lobo
Departament de Fisica Fonamental, Universitat de Barcelona, Barcelona, Spain
(Received 17 September 1992)

We propose a new method of operating laser interferometric gravitational-wave detectors when observing *chirps* of gravitational radiation from coalescing compact binary stars. This technique consists of the use of narrow-band dual recycling to increase the signal but with the tuning frequency of the detector arranged to follow the frequency of a chirp. We consider the response of such an instrument to chirps, including the effect of inevitable errors in tracking. Different possible tuning strategies are discussed. Both the final signal-to-noise ratio and timing accuracy are evaluated and are shown to be significantly improved by the use of dynamic tuning. This should allow an accurate and reliable measurement of Hubble's constant.

PACS number(s): 04.80.+z, 07.60.Ly, 95.85.Sz, 98.80.Es

I. INTRODUCTION

The new generation of laser interferometric gravitational-wave detectors may revolutionize the way in which we observe the Universe [1]. A particularly useful type of gravitational radiation may well be that emitted as two neutron stars or black holes in a binary system spiral in towards each other. With a few percent of the rest mass of the binary being radiated as gravitational waves, and with the predictable waveform allowing the use of matched filtering, these events should be observable out to great distances. The estimated coalescence event rate is about three per year out to 100 Mpc [2], at which distance typical signal-to-noise ratios might be ~ 10 for broadband detectors operating at their design sensitivity [3,4]. A total of ~ 50 chirps per year might be seen by a network of three or four such detectors. Schutz [5] has proposed that the cosmological distance scale (Hubble's constant H_0) might be determined in a new and potentially accurate way by observation of the chirp of gravitational waves emitted in the final few seconds of the life of these compact binaries. The distance of the source may be found from a combination of the amplitude and rate of change of frequency of the chirp:

$$\langle h \rangle = 10^{-23}\, \mathcal{M}_{\odot}^{5/3} f_{100}^{2/3} r_{100}^{-1} \tag{1}$$

and

$$\dot{f} = 13\, \mathcal{M}_{\odot}^{5/3} f_{100}^{11/3}\ \mathrm{Hz\,s^{-1}}\ , \tag{2}$$

where the binary mass parameter $\mathcal{M}_{\odot}^{5/3} = \mu M_{\mathrm{tot}}^{2/3}$, μ and M_{tot} being the reduced and total masses in units of the solar mass; f_{100} is the gravitational wave frequency in units of 100 Hz and r_{100} is the source distance in units of 100 Mpc; $\langle h \rangle$ is the rms signal amplitude averaged over detector orientation and polarization, measurable by three detectors [5]. With a measurement of $\dot{f}$ giving the chirp mass parameter, measurement of $\langle h \rangle$ gives the distance to the binary. If the source can be identified with a particular cluster of galaxies, then its redshift may be measured. The combination of a distance and a redshift, measured at typical distances of ≥ 100 Mpc where the random velocities are small compared to the Hubble flow, will give in one step a value of Hubble's constant.

While a statistical determination of H_0 is possible with modest directional accuracy [5], it is desirable to be able to identify the source of gravitational waves with either a single galaxy or a single cluster of galaxies. This requires positional accuracy of better than $\sim 0.5/r_{100}$ degrees [6]. The position of the source is determined by measuring the differences in the times of arrival of a chirp at the different detectors in a worldwide network. If the separation of two detectors is d and the angle of the source relative to the line between them is θ, then the time delay τ_{12} between the arrival of the signal at the two detectors is just

$$\tau_{12} = d\cos\theta / c\ , \tag{3}$$

c being the speed of both light and the gravitational waves. So if we want to measure the position to an accuracy $\Delta\theta$, the delay must be known to within

$$\Delta\tau_{12} < 0.1 \left[\frac{d}{5\times 10^3\ \mathrm{km}}\right]\left[\frac{\Delta\theta}{0.5^\circ}\right]\left[\frac{\sin\theta}{0.5}\right]\ \mathrm{ms}\ . \tag{4}$$

*Deceased.

With such high accuracy required, prospects for a rapid and clean measurement will be enhanced if the detectors can be arranged to reduce as much as possible the errors in estimating the properties of the signal. We will discuss one way in which this may be achieved.

Laser interferometric gravitational wave detectors work by letting the fluctuating spacetime curvature of a gravitational wave induce a change in phase upon a beam of light. The phase change is then converted into an observable change in power by interference with a different light beam. The size of the signal is increased by allowing the light and the gravitational wave to interact for the maximum possible time. While the light power may be recycled so that it has a long interaction time [7], best performance of a broadband detector is obtained if the signal (sidebands) are extracted after approximately half the period of the gravitational waves. This limits the signal buildup at each frequency. However, the signal may be further enhanced within a restricted bandwidth if it is arranged that the phase change induced on the light at one time always adds to that induced at other times. Originally suggested by Drever [7], there is a flexible variant of this known as *dual recycling,* proposed by one of us [8], that has been experimentally demonstrated [9] recently. The optical arrangement of dual recycling is indicated in Fig. 1. Note that the tuning frequency, being determined by the position of the signal recycling mirror M_3, is quite easily adjustable and that the signal enhancement is almost independent of the tuning frequency.

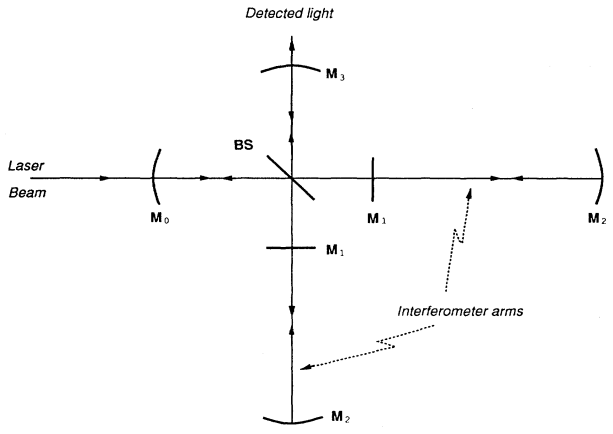

FIG. 1. The optical layout of an interferometer using dual recycling. Differential phase shifts between the two arms of the interferometer change the power of the output light, the phase shifts being increased in practice by multiple traverses of each arm. With the interferometer on a dark fringe, most of the light is directed back towards the laser, is caught by the power recycling mirror M_0, and added coherently to the incoming laser light. The partially transmitting signal recycling mirror M_3 is placed at the output to resonate signal sidebands induced by a gravitational wave. It is always possible to find a position of M_3 such that at least one signal sideband will, when reflected back in, add coherently with the sideband that is then being generated by a gravitational wave. So the position of M_3 determines the tuning frequency of the detector, while the transmission of M_3 determines the signal interaction time and hence, the bandwidth.

This recycling of the signal improves the narrow-band sensitivity as the square root of the factor by which the bandwidth is reduced, limited by the losses of the system. The improvement factor, compared with a previously optimized broadband interferometer, can be an order of magnitude at gravitational wave frequencies of a few hundred hertz [8]. Is there some way in which we can take advantage of this for sources emitting over a wide frequency range? It is already known that the signal-to-noise ratio (S/N) for the detection of pulses is about the same with a narrow-band as with a broadband system [8], and that for chirp detection may even be a factor of ~ 1.5 greater in narrow-band operation [4]. But information about most of the frequency components contained in the signal is being thrown away if we narrow band, which is clearly not ideal if we wish to extract as much knowledge as possible from the detection. For example, the best possible timing accuracy, with an effective bandwidth Δf (determined by a combination of the signal spectrum and the detector response), is

$$\Delta t \approx [\Delta f (S/N)]^{-1} . \tag{5}$$

So both broad bandwidth and high signal-to-noise ratio are important. It appears that there are two contradictory requirements: attainment of the highest signal level at a given frequency seems to need narrow banding, but observation of all of the frequency components requires a detector spanning a broad frequency range. However, a chirp is rather special: it can be approximated as a sine wave which continually increases in frequency as the two stars spiral in towards each other. We can imagine *dynamically tuning* the interferometer so that the frequency at which the detector response is best coincides with that of the gravitational waves. This would entail adjusting the position of the signal recycling mirror M_3 to keep within the detector bandwidth.[1] If this is possible, the sensitivity of the detector would always be near optimal and all of the signal frequency components would be observed. We would therefore expect that both the S/N and the accuracy of estimating the arrival time and rate of change of frequency of the chirp, would be increased by a factor corresponding to the gain in signal going from a broadband to a narrow-band system.

This improvement in performance can only be obtained, of course, if it is possible to track the evolving gravitational wave with the detector. Perhaps the simplest way that we might imagine doing this would be to operate a narrow-band interferometer at a tuning frequency of, say, 100 Hz (below which other noise would be prohibitive [1,3]), wait for a chirp to traverse the detector passband, measure the rate of change of frequency and arrival time, then adjust the tuning frequency to follow the signal. This has to be done well enough that the signal lies within the detector bandwidth up to the maximum observing frequency $f_{\max}$. A choice of $f_{\max} \approx 500$ Hz seems sensible since there is little signal power at

[1]Roland Schilling has told us that Peter Kafka has also suggested this idea.

higher frequencies, but the wave form may be distorted by either tidal interactions or post-Newtonian effects [10].

In order to be able to asses the feasibility of this, an understanding is required of how the signal buildup and the final errors in estimating the chirp parameters are affected by errors in tuning. We need to calculate not only the response of a dynamically tuned detector but also how well the future frequency evolution of a chirp may be estimated from an initial narrow-band detection. We will consider each of these two different aspects of the problem in turn, then bring them together in Sec. V, where we shall discuss the potential improvement in both signal-to-noise ratio and parameter accuracy by the use of dynamic tuning.

II. DETECTOR RESPONSE

We need to derive the response of a dynamically tuned laser interferometer to a chirp of gravitational radiation. A calculation of the output wave form will allow evaluation of the signal-to-noise ratio and of the accuracy of estimating the parameters of the chirp. The derivation will follow the approach taken in Ref. [11]. The difference is that both the gravitational-wave and the detector tuning frequencies can be functions of time t. The aim is to calculate the observed power change produced by the gravitational waves, proportional to the sideband amplitude emerging from the detector.

The gravitational-wave chirp emitted by a coalescing binary as a sine wave of continually increasing angular frequency ω, with amplitude

$$h=h_0(t)\cos\Phi(t), \quad \Phi(t)=-\int_0^t \omega(t')dt' . \tag{6}$$

We will assume a round trip time τ for the light in the arms of the interferometer such that $\omega\tau \ll 1$ and $\dot{\omega}\tau^2 \ll 1$. This is a good approximation for currently conceived detectors and chirps. The frequency of the gravitational wave at time $t-\tau$ will then be

$$\omega(t-\tau)\approx\omega(t)-\dot{\omega}(t)\tau , \tag{7}$$

and the corresponding phase Φ of the gravitational wave will be

$$\Phi(t-\tau)=\int_0^\tau \omega(t-\tau')d\tau'\approx\omega(t)\tau-\tfrac{1}{2}\dot{\omega}(t)\tau^2 . \tag{8}$$

The differential phase change $\delta\phi$ induced on light of angular frequency ω_L by the gravitational wave on a single round trip of the interferometer will be [11, 17]

$$\delta\phi\approx\tfrac{1}{2}h_0\tau\omega_L(e^{i\omega t}+e^{-i\omega t}) . \tag{9}$$

Since a phase shift $\delta\phi$ effectively multiplies the field of the laser light by $e^{i\delta\phi}\approx 1+i\delta\phi$, it can be seen that two sidebands are imposed on the light by the signal. We need to add the signal sidebands generated throughout the history of the light. If the recycling cavity is on resonance, the amplitude E_+ of the *plus* sideband emerging from the interferometer is

$$\frac{E_+}{E_0}\approx\frac{iT_{1c}T_{1s}R_2h_0\tau\omega_L}{4(1-R_{1c}R_2)}[e^{i\delta_s(t)}e^{i\omega(t)t}+R_{1s}R_2e^{i\delta_s(t-\tau)}e^{i\omega(t-\tau)}e^{i\Phi(t-\tau)}e^{i\delta_s(t)}+\cdots] , \tag{10}$$

with E_0 the rms amplitude of the incident laser light. The phase offset $\delta_s(t)$ in the signal recycling cavity determines the tuning of the detector. Now $e^{i\omega(t-n\tau)t}$ will contain an $e^{i\omega n\tau t}$ term. Fortunately, however, the fairly slow change in frequency of the chirp means that we can neglect this term in practice. For realistic sweep times ξ and signal storage times τ_2, it is true that

$$\dot{\omega}(t)\tau_s \ll \omega(t) . \tag{11}$$

Equivalently, the detector bandwidth B must satisfy the condition that

$$B \gg 0.04\,\mathcal{M}_\odot^{5/3}f_{100}^{8/3}\ \text{Hz} . \tag{12}$$

We may also write

$$\delta_s(t-\tau)\approx\delta_s(t)-\dot{\delta}_s(t)\tau . \tag{13}$$

With this simplification the emerging sideband field is

$$\frac{E_+}{E_0}\approx\frac{iT_{1c}T_{1s}R_2h_0\tau\omega_L}{4(1-R_{1c}R_2)}e^{i\delta_s(t)}e^{i\omega t}\sum_{n=0}^{\infty}(R_{1s}R_2)^n e^{-in(\omega\tau-\delta_s+\dot{\delta}_s\tau)}e^{i(\dot{\omega}\tau-\dot{\delta}_s)n^2\tau/2} . \tag{14}$$

The sum over the number of bounces may be converted to an integral over time:

$$\frac{E_+}{E_0}\approx\frac{iT_{1c}T_{1s}R_2h_0\omega_L}{4(1-R_{1c}R_2)}e^{i\delta_s}e^{i\omega t}\int_0^\infty(R_{1s}R_2)^{t'/\tau}e^{-i(t'/\tau)(\omega\tau-\delta_s+\dot{\delta}_s\tau)}e^{i(\dot{\omega}\tau-\dot{\delta}_s)(t'/\tau)^2\tau/2}dt' . \tag{15}$$

Using $(t'/\tau)\ln R_{1s}R_2=t'/\tau_s$ and normalizing the time variable to the signal storage time $s=t'/\tau_s$ enables us to write this as

$$\frac{E_+}{E_0}\approx\frac{iT_{1c}T_{1s}R_2h_0\omega_L\tau_s}{4(1-R_{1c}R_2)}e^{i\delta_s}e^{i\omega t}\mathcal{J}_s , \tag{16}$$

where the integral $\mathcal{I}_s$ is given by

$$\mathcal{I}_s=\int_0^\infty \exp\{-s-i[s\tau_s(\omega-\delta_s/\tau+\dot{\delta}_s)+s^2(\dot{\omega}-\dot{\delta}_s/\tau)\tau_s^2/2]\}ds\ . \tag{17}$$

Note the form of the integral: the $(\omega-\delta_s/\tau)$ term represents a tuning offset between the gravitational wave and the interferometer. If this is small the sidebands add up in phase, the integral is real and equal to unity, and we recover the result for the buildup of a static signal. There is a further condition for efficient signal buildup, that the frequency must not change too quickly:

$$\dot{\delta}_s/(\pi B)\ll 1\ . \tag{18}$$

If $\omega=\delta_s/\tau$ then this may be written as

$$B\gg 5\times 10^{-4}\left[\frac{\tau}{2\times 10^{-5}\,\mathrm{s}}\right]\mathcal{M}_\odot^{5/3}f_{100}^{11/3}\ \mathrm{Hz}\ , \tag{19}$$

where the value of the round trip time in the detector arms $\tau=2\times 10^{-5}$ s is appropriate to a 3 km cavity interferometer (a multipass delay line would behave similarly if tuning was implemented via the mirrors in the interferometer arms rather than just the signal recycling mirror). Since the bandwidth that gives maximum signal buildup is about 1.6 Hz for such an instrument, the response of a perfectly tracked dynamically tuned interferometer is near optimal over a considerable range of masses and frequencies. In situations in which the rate of change of frequency or the tuning offset are significant, the response integral may be done numerically.

The chirp changes its frequency at a rate described by Eq. (2). Alternatively, the time t_{12} taken for the chirp frequency to evolve from frequency f_{100_1} to f_{100_2} is

$$t_{12}=\frac{3}{\mathcal{M}_\odot^{5/3}}\left[\frac{1}{f_{100_1}^{8/3}}-\frac{1}{f_{100_2}^{8/3}}\right]\ \mathrm{s}\ . \tag{20}$$

So a measurement of the mass parameter $\mathcal{M}_\odot$ by an observation of the chirp at a certain frequency and time can give an estimation of the chirp frequency f_{100} at later times. If the detector is tuned to a frequency f_{T100} having the same form as f_{100}, so that $\delta_s=200\pi\tau f_{T100}$, then substituting into our integral for the signal gives

$$\mathcal{I}_s=\int_0^\infty \exp\left\{-s-i\left[\frac{200(f_{100}-f_{T100}-0.13\tau\mathcal{M}_\odot^{5/3}f_{100}^{11/3})s}{B}-\frac{4s^2\mathcal{M}_\odot^{5/3}(f_{100}^{11/3}-f_{T100}^{11/3})}{B^2}\right]\right\}ds\ . \tag{21}$$

We need to calculate the observable output signal, a change in light power δI produced by beating the sidebands with a local oscillator field [11] E_L:

$$\delta I=E_LE_+^*+E_LE_-^*+E_L^*E_++E_L^*E_-\ , \tag{22}$$

where an asterisk indicates complex conjugation. If we maintain our concentration on a single sideband, write $\mathcal{T}=T_{1c}/(1-R_{1c}R_2)$ and use

$$T_{1s}\tau_s=\frac{T_{1s}}{\pi B}=\frac{(2\pi\tau B-NA^2)^{1/2}}{\pi B}\ , \tag{23}$$

where NA^2 are the overall losses in the arms of the interferometer, then we obtain

$$|\delta I(t)|\approx\frac{E_0E_L\mathcal{T}h_0\omega_L(2\pi\tau B-NA^2)^{1/2}}{2\pi B}|\mathcal{I}_s|\ . \tag{24}$$

So we now have an expression for the intensity change at each frequency produced by the chirp. This signal wave form can be related simply to the root spectral density $\tilde{\delta}I(f)$ of the signal [12]:

$$|\tilde{\delta}I(f)|=\frac{\delta I(t)}{\sqrt{4\dot{f}}} \tag{25}$$

for a slowly varying frequency. It is this signal spectral density, together with that of noise, that is needed to calculate the information extractable from an observation. For example, the optimum signal-to-noise ratio may be calculated using the standard formula (e.g., [1])

$$(S/N)^2=2\int_0^\infty\frac{|\delta\tilde{I}(f)|^2}{|\delta\tilde{I}_n(f)|^2}df \tag{26}$$

Throughout this paper we shall make the simplifying assumption that the detector noise $|\delta\tilde{I}_n|$ is dominated, above a seismic cutoff frequency that we take as 100 Hz, by the photon shot noise of the coherent local oscillator field. We shall consistently neglect extra noise resulting from poor fringe contrast or any other source (see, e.g., Refs. [13,1,3] for a discussion of this). So the noise has a root spectral density [14]

$$|\delta\tilde{I}_n(f)|=(2E_L^2\hbar\omega_L)^{1/2}\ , \tag{27}$$

giving

$$(S/N)^2=\frac{2.1\times 10^{-4}\mathcal{T}^2I_0\mathcal{M}_\odot^{5/3}}{\lambda_Lr_{100}^2}\times\int_{f_{\min_{100}}}^{f_{\max_{100}}}\frac{2\pi\tau B-NA^2}{B^2f_{100}^{7/3}}|\mathcal{I}_s|^2df_{100}\ , \tag{28}$$

with λ_L the wavelength of the light in the interferometer. The expression (1) for the averaged gravitational wave amplitude has been used here, so that S/N is the average value for a network. Favorable orientation of source and

detector would give values of S/N higher by $\sqrt{5}$. If the power buildup within the recycling system is limited by the mirror losses and the transmission of the power recycling mirror is optimized, then the recycling factor $\mathcal{F}$ takes its maximum value.

$$\mathcal{F}=1/\sqrt{NA^2}\ . \tag{29}$$

In this optimum case we can write the typical S/N with dynamic tuning as

$$S/N=221\left[\frac{I_0}{50\ \mathrm{W}}\right]^{1/2}\left[\frac{\lambda_L}{0.5\ \mu\mathrm{m}}\right]^{-1/2}\mathcal{M}_{\odot}^{5/6}r_{100}^{-1}\mathcal{J}_{dt}\ , \tag{30}$$

where the factor $\mathcal{J}_{dt}$ is given by

$$\mathcal{J}_{dt}\equiv\left\{\int_{f_{100\,\mathrm{min}}}^{f_{100\,\mathrm{max}}}\left[\frac{(2\pi lB/cA^2)-1}{B^2f_{100}^{7/3}}\right]|\mathcal{I}_s|^2\,df_{100}\right\}^{1/2}, \tag{31}$$

with l the armlength of the interferometer. This result is independent of whether cavities or delay lines are used as multiple reflection systems within the arms of the interferometer, as long as the upper observing frequency is well below the first zero in the detector frequency response. This should be a good approximation in practice. The size of $\mathcal{J}_{dt}$ determines the signal-to-noise ratio that may be obtained with a particular detector arrangement. The maximum value of $\mathcal{J}_{dt}$ is

$$\mathcal{J}_{dt}(\mathrm{max})\approx 0.51\ , \tag{32}$$

assuming a perfectly tracked slowly changing chirp (for which $|\mathcal{I}_s|^2=1$) observed between 100 Hz and 500 Hz with an interferometer having arms 3 km in length and $A^2=5\times10^{-5}$. We will discuss further the possible magnitude of $\mathcal{J}_{dt}$ in Sec. V, but we can see already that dynamic tuning has the potential to increase the signal-to-noise ratio of a chirp by a factor ~ 15 over that possible with an optimized broadband detector.

For a "conventional" narrow-band detector, in which only one sideband is resonant, it is a very good approximation to neglect one sideband. There are at least two situations, however, in which the effect of both sidebands needs to be included. One such case is simply if the bandwidth during any part of the observation is sufficiently broad for the contribution from the other sideband to be significant. Both signal sidebands must also be included if the optical arrangement used is designed so that two sidebands are simultaneously resonant. Such a system, doubly resonant signal recycling, has been proposed recently [15]. This uses a long storage time cavity as a frequency-dependent signal recycling mirror, splitting the resonance of the signal recycling cavity. The action of the frequency-dependent mirror is to produce a different phase shift on reflection for the two sidebands. The resultant difference in phase shift δ_s per round trip of the signal recycling cavity allows two sidebands to be resonant. The frequency response of a doubly resonant detector is modified in such a way that the peak signal of an instrument with the same bandwidth as a corresponding singly resonant detector is increased by a factor of $\sqrt{2}$. Alternatively, a doubly resonant detector with the same peak response has twice the bandwidth. With this modification, the rest of the analysis remains unchanged. Thus, while we shall quote results for a singly resonant interferometer, signal-to-noise ratios and parameter accuracies can be improved by a further factor of $\sqrt{2}$ by the use of doubly resonant signal recycling.

If we wish to explicitly include both sidebands, then we can keep the expressions for the two amplitudes in formula (22) for the power change. The maximum power change occurs when all three phasors (E_L,E_+, and E_-) are parallel at one point of the cycle. This is when the phase Ψ for the local oscillator field and the time t_0 (modulo $1/f$) are given by

$$\Psi=-\omega t_0=\tfrac{1}{2}\{\arg[E_+e^{-i\omega t}]+\arg[E_-e^{i\omega t}]\}\ . \tag{33}$$

The control system for the local oscillator phase will almost certainly not sense the gravitational wave itself but an artificial signal that should behave in a similar way. For example, the length of the interferometer atoms might be differently modulated at a frequency equal to the gravitational-wave frequency plus a free-spectral range of the signal recycling cavity. The local oscillator phase Ψ would then be adjusted to maximize the size of this perfectly resonant artificial signal. This would be a slightly different phase from that required to maximize a signal that is not quite on resonance. So the values of E_+ and E_- used to calculate Ψ should assume perfect tuning. We can then calculate the waveform seen by the photodetector.

We did not worry about the local oscillator phase in the single sideband case. The magnitude of the beat signal is then independent of the local oscillator phase; only the best demodulation phase would change. It would be possible to demodulate the signal twice, with quadrature phase. A linear combination, defined by the tuning, would allow reconstruction of the signal and attainment of the best S/N.

We now have the ability to calculate the output waveform of a dynamically tuned interferometer. This enables us to determine the final signal-to-noise ratio and the errors in the measurement of the chirp parameters if we know how accurately the chirp can be tracked.

III. ESTIMATION OF CHIRP PARAMETERS

In a companion paper [16] (henceforth referred to as paper I) we discuss the general problem of estimating the time of arrival and mass parameter of a chirp of gravitational radiation. Here we will quickly summarize the results that we will need in order both to assess how accurately a chirp may be tracked by a dynamically tuned interferometer, and also to calculate the uncertainty in the final estimation of the chirp amplitude and mass (hence distance), and arrival time (hence position).

In general, the final errors in the chirp parameters are

given by components of the covariance matrix, the inverse of the information matrix [16]. This complication is necessary because uncertainty in the mass, for example, produces uncertainty in the arrival time. One simplification is that it is possible to explicitly eliminate consideration of the phase of the signal [16], reducing the information matrix to a symmetric two-dimensional form, with components

$$\Gamma_{tt}=2\int_{f_{\min}}^{f_{\max}}\frac{(2\pi f)^2|\tilde{\delta}I(f)|^2}{|\delta\tilde{I}_n(f)|^2}df-\frac{2\left[\int_{f_{\min}}^{f_{\max}}\frac{(2\pi f)|\tilde{\delta}I(f)|^2}{|\delta\tilde{I}_n(f)|^2}df\right]^2}{\int_{f_{\min}}^{f_{\max}}\frac{|\tilde{\delta}I(f)|^2}{|\delta\tilde{I}_n(f)|^2}df}\ , \tag{34}$$

$$\Gamma_{tm}=2\int_{f_{\min}}^{f_{\max}}\frac{(2\pi f)a(f)|\tilde{\delta}I(f)|^2}{|\delta\tilde{I}_n(f)|^2}df-\frac{2\left[\int_{f_{\min}}^{f_{\max}}\frac{(2\pi f)|\tilde{\delta}I(f)|^2}{|\delta\tilde{I}_n(f)|^2}df\right]\left[\int_{f_{\min}}^{f_{\max}}\frac{a(f)|\tilde{\delta}I(f)|^2}{|\delta\tilde{I}_n(f)|^2}df\right]}{\int_{f_{\min}}^{f_{\max}}\frac{|\tilde{\delta}I(f)|^2}{|\delta\tilde{I}_n(f)|^2}df}\ , \tag{35}$$

and

$$\Gamma_{mm}=2\int_{f_{\min}}^{f_{\max}}\frac{a^2(f)|\tilde{\delta}I(f)|^2}{|\delta\tilde{I}_n(f)|^2}df-\frac{2\left[\int_{f_{\min}}^{f_{\max}}\frac{a(f)|\tilde{\delta}I(f)|^2}{|\delta\tilde{I}_n(f)|^2}df\right]^2}{\int_{f_{\min}}^{f_{\max}}\frac{|\tilde{\delta}I(f)|^2}{|\delta\tilde{I}_n(f)|^2}df}\ , \tag{36}$$

with

$$a(f_{100})=530\,\mathcal{M}_{\odot}^{-10/3}(3f_{10}^{-5/3}+5f_{100}-8)\ . \tag{37}$$

Since the inverse of this two-dimensional matrix is the covariance matrix, the error $\Delta\mathcal{M}_{\odot}$ in estimating the mass parameter is given by

$$\Delta\mathcal{M}_{\odot}^{5/3}=\left[\frac{\Gamma_{tt}}{\Gamma_{mm}\Gamma_{tt}-\Gamma_{tm}^2}\right]^{1/2}, \tag{38}$$

while the uncertainty Δt_i in the time of arrival of the chirp at an individual detector is

$$\Delta t_i=\left[\frac{\Gamma_{mm}}{\Gamma_{mm}\Gamma_{tt}-\Gamma_{tm}^2}\right]^{1/2}. \tag{39}$$

The minimum uncertainty in the amplitude of the gravitational wave is simply determined by the signal-to-noise ratio, given by Eqs. (26) and (30):

$$\frac{\Delta h}{h}=\frac{1}{S/N}\ . \tag{40}$$

The uncertainty Δr_{100} in the distance to the coalescing binary (in 100 Mpc) may then be found by combining the expression (1) for the gravitational wave amplitude with those for the uncertainty in mass (38) and amplitude (40). This gives

$$\frac{\Delta r_{100}}{r_{100}}=\left[\left[\frac{1}{S/N}\right]^2+\left[\frac{\Delta\mathcal{M}_{\odot}^{5/3}}{\mathcal{M}_{\odot}^{5/3}}\right]^2\right]^{1/2}. \tag{41}$$

It should be stressed that the errors given by these expressions are the best possible ones, with optimum data analysis. Since the analysis does not have to take place in real time, plenty of computing power should be available and these minimum errors should be attainable. A possible exception is the error for the distance to the source, the measurement of which requires amplitudes from different detectors in a network to be combined. Inevitable differences in detector calibration will probably limit distance measurements to accuracies of a few percent.

The estimate of the time of arrival of a chirp at an individual detector is degraded by the uncertainty in the mass and phase of the chirp. But if the same chirp is seen by a network of detectors it is known that the mass parameter is common to them all and there is a well-defined phase difference between each of the instruments. For example, if the detectors have the same orientation, the signal must have identical mass parameter and phase in all of the instruments. So, while the problem with arbitrary detector orientations is currently being studied [18], it seems likely that the result for the errors in the time delay between different detectors is particularly simple, reducing to the case in which only one parameter is unknown (cf. paper I). The variance C_{tt} in the relative timing is then given by

$$\frac{1}{C_{tt}}=2\int_{f_{\min}}^{f_{\max}}\frac{(2\pi f)^2|\tilde{\delta}I(f)|^2}{|\delta\tilde{I}_n(f)|^2}df\ . \tag{42}$$

So the final relative timing error Δt_{dt} is

$$\Delta t_{dt}=0.018\left[\frac{I_0}{50\ \mathrm{W}}\right]^{-1/2}\left[\frac{\lambda_L}{0.5\ \mu\mathrm{m}}\right]^{1/2}\times\mathcal{M}_{\odot}^{-5/6}r_{100}\mathcal{H}_{dt}^{-1}\ \mathrm{ms}\ , \tag{43}$$

where the factor $\mathcal{K}_{dt}$ is given by

$$\mathcal{K}_{dt} \equiv \left\{ \int_{f_{100_{\min}}}^{f_{100_{\max}}} \left[\frac{(2\pi lB/cA^2)-1}{B^2 f_{100}^{1/3}} \right] |\mathcal{I}_s|^2 \, df_{100} \right\}^{1/2} . \tag{44}$$

$\mathcal{K}_{dt}$ is similar to the equivalent integral $\mathcal{I}_{dt}$ for the signal-to-noise ratio (31), but it has a weaker frequency dependence and so a higher value. For example, $\mathcal{K}_{dt}^{-1} \approx 0.94$ for a perfectly tracked chirp observed between 100 and 500 Hz with $l=3$ km, $B=1.6$ Hz, and $A^2=5\times10^{-5}$. So a very good timing accuracy of ~ 0.02 ms seems possible. This may be converted into an approximate positional accuracy by reference to Eq. (4).

IV. TRACKING A CHIRP

If the final signal-to-noise ratio and the estimates of the source position and distance are to approach their optimal values, then the tuning frequency of the detector must follow that of the gravitational waves quite accurately. At least one sideband induced by the gravitational wave must be resonant up to the maximum observing frequency $f_{\max}$. We shall illustrate further the effect of imperfect tuning in Sec. V, but it is instructive to try and estimate the required accuracy for both the chirp timing and mass parameter.

Any error Δt in the time at which tracking starts must be less than the time it takes for the chirp to traverse the detector bandwidth, $\Delta t < B/\dot{f}_{\max}$. Since the rate of change of the chirp frequency is given by (2), the timing constraint is

$$\Delta t < \frac{B(f)}{13\,\mathcal{M}_\odot^{5/3} f_{100}^{11/3}} \approx 5\times10^{-3} \left[\frac{B}{10\text{ Hz}} \right] \left[\frac{f}{400\text{ Hz}} \right]^{-11/3} \mathcal{M}_\odot^{-5/3} \text{ s} . \tag{45}$$

Remember that the bandwidth *can* be a function of frequency: if a cavity is used as the signal recycling mirror its transmission and hence the bandwidth may be varied by adjusting the cavity tuning [8,14].

The gravitational-wave frequency is given by Eq. (20). If this frequency is to be within an optical bandwidth of the detector tuning frequency, then the mass parameter must be estimated to an accuracy

$$\frac{\Delta\mathcal{M}_\odot^{5/3}}{\mathcal{M}_\odot^{5/3}} < 2.7\times10^{-2} B f_{100_2}^{-11.3} \left[\frac{1}{f_{100_1}^{8/3}} - \frac{1}{f_{100_2}^{8/3}} \right]^{-1} . \tag{46}$$

Note how the frequency error builds up after the initial estimation at f_{100_1}. If we take this initial frequency as 100 Hz then at significantly higher frequencies $f_{100_1}^{-8.3} \gg f_{100_2}^{-8/3}$ and we can write

$$\frac{\Delta\mathcal{M}_\odot^{5/3}}{\mathcal{M}_\odot^{5/3}} < 2\times10^{-3} \left[\frac{B}{10\text{ Hz}} \right] \left[\frac{f}{400\text{ Hz}} \right]^{-11/3} . \tag{47}$$

So the required accuracy of both the timing and the frequency sweep rate gets much tougher at high signal frequencies.

If dynamic tuning is to work, the presence of a possible chirp must first be detected by a narrow-band interferometer tuned to as low a frequency as possible. We shall take this initial frequency to be 100 Hz. Because the signal power is greater at low frequencies, the signal-to-noise ratio in such a narrow-band instrument may actually be larger than that obtainable in a broadband detector, the improvement factor being ~ 1.5 with a bandwidth B of 6 Hz [5]. The output signal from the narrow-band detector must be analyzed promptly, in real time, to detect the candidate chirp and to initiate the dynamically tuned phase. There are then a range of strategies, depending on the sophistication of the data analysis, that can be employed to ensure that the tuning is accurate. By far the crudest is to make no attempt at all to estimate the mass parameter of the chirp other than guess that the binary consists of two 1.4 $\mathcal{M}_\odot$ neutron stars. While this will probably be quite close to being correct most of the time, it will occasionally be drastically wrong. It will be better to use the detector output to estimate the mass parameter and arrival time. The best possible accuracy of measuring the mass parameter with a static narrow-band system is [17]

$$\frac{\Delta\mathcal{M}_\odot^{5/3}}{\mathcal{M}_\odot^{5/3}} \approx 0.1 \left[\frac{10\text{ Hz}}{B} \right]^2 \left[\frac{4}{(S/N)_i} \right] \mathcal{M}_\odot^{5/3} , \tag{48}$$

while the arrival time of chirp at the reference frequency 100 Hz may be estimated to

$$\Delta t \approx 2.5\times10^{-2} \left[\frac{10\text{ Hz}}{B} \right] \left[\frac{4}{(S/N)_i} \right] \text{ s} , \tag{49}$$

with the approximations good for initial signal-to-noise $(S/N)_i > 3$. It can be seen that estimation of the chirp parameters only from an initial narrow-band detection would be adequate for dynamic tuning up to about 200 Hz with a fixed bandwidth of 15 Hz and an initial signal-to-noise ratio as low as 4. Accurate tuning to even higher frequencies is then possible either if the bandwidth is increased at high frequencies or if the parameter estimation is continually refined during the dynamic phase.

The optimal strategy is hard to judge at this point in time, but we shall describe one possibility. This starts by making the initial detection with quite a narrow-band system, perhaps $B \sim 6$ Hz. While such a system has fairly poor mass and timing discrimination, the small frequency range over which the chirp evolves during its passage through the bandwidth of the detector means that this accuracy may be adequate to ensure that the detector tuning can follow the chirp for the next few Hz, at least. The relatively small amount of data associated with the low bandwidth, together with the rather crude estimation required, also eases the computing power needed for the prompt data analysis. Once the chirp frequency has evolved somewhat further, with the detector tracking it, the output of the detector may be reanalyzed and a new estimation of the chirp parameters made. The tuning may then be readjusted so that the detector may continue to follow the gravitational wave frequency with sufficient accuracy. This process may be repeated throughout the

evolution of the chirp. The data analysis is made easier at each stage by the previous knowledge of the chirp parameters; it is a zooming in on the correct values. In principle, this scheme could give very small tuning errors, essentially given at each stage by Eqs. (38) and (39). We shall give examples for the possible signal-to-noise ratio and parameter accuracies in Sec. V.

That there is enough information in an initial narrow-band detection to successfully start dynamic tuning with later updating may be seen by combining the expressions (45) and (46) for the required parameter accuracy with (49) and (48) for the possible accuracy from the initial detection. If we demand, say, that after the chirp has evolved by about a bandwidth B its frequency must be still within B of the tuning frequency, the bandwidth is constrained by

$$B > 3\left[\frac{4}{(S/N)_i}\right]^{1/2}\mathcal{M}_\odot^{5/6}\ \text{Hz}\ . \tag{50}$$

So, even with low initial signal-to-noise ratios $(S/N)_i$, it is possible to use quite narrow bandwidths and take advantage of the associated high signal buildup.

There is an additional constraint on the lowest threshold that can be used to start the dynamically tuned phase. This is simply that the detector should not spend a significant fraction of its time triggering on noise. If decisions whether to trigger or not are made at time intervals t_d and the threshold for triggering is T times the rms noise (which we assume to be Gaussian), then the typical time interval t_t between triggering on noise is

$$t_t = \frac{t_d}{\text{erfc}(T)}\ , \tag{51}$$

where erfc(T) is the complementary error function. If t_d was 100 ms, reasonable for a narrow-band system, a threshold for initial detection of 3 would lead to the detector triggering on noise every eight minutes or so, while $T=4$ would give $T_t \sim 80$ days. Each false trigger would put the detector out of action for the time scale of a chirp, a few seconds. So it may be possible to operate dynamic tuning with initial signal-to-noise ratios in a narrow-band instrument as low as 3. This would correspond to $S/N \sim 2$ in a broadband detector [5]. These low S/N candidate events would then be confirmed or denied as chirps by the enhancement of S/N during the dynamically tuned phase. With typical thresholds for a broadband system being $T_{\text{bb}} \sim 4.5$, the number of events observable by a dynamically tuned interferometer might be higher by a factor $(4.5/2)^3 \approx 10$.

Another important practical question is the feasibility of adjusting the position of the signal recycling mirror with sufficient accuracy and speed to ensure good signal buildup at all frequencies. The actual motion of the signal recyclying mirror is only a small fraction ($\sim 10^{-2}$) of a wavelength, so this is no problem. The tuning of the signal recycling cavity will be controlled by a feedback system which will maintain efficient resonance at the estimated signal frequency. It is straightforward to convert an estimate of the correct tuning into a position of the signal recycling mirror, by shifting the frequency of a control beam, for example [9]. The control system must have enough bandwidth to be able to follow the evolution of the chirp. This is easy at low frequencies, at which the chirp frequency changes with a timescale of seconds, but gets rapidly more difficult at high frequencies. The characteristic frequency (inverse timescale) at which the chirp evolves is

$$\frac{\dot{f}}{f} \approx 5\,\mathcal{M}_\odot^{5/3}\left[\frac{f}{400\ \text{Hz}}\right]^{8/3}\ \text{Hz}\ . \tag{52}$$

The feedback gain at this frequency must be high enough to keep the tuning to within an optical bandwidth of the desired frequency. It will be sensible to use the signal representing the estimate of the correct tuning frequency to directly move the signal recycling mirror as well as to alter the frequency of the oscillator determining the resonant frequency of the signal recycling cavity. This will reduce the frequency error seen by the control system by a factor η that depends on how well the calibration of the transducer that moves the signal recycling mirror is known. If we consider only a simple, unconditionally stable servo system with unity gain frequency f_{ser}, then the requirement is that

$$\frac{f_{\text{ser}}}{f} > 0.01\,\mathcal{M}_\odot^{5/3}\left[\frac{B}{4\ \text{Hz}}\right]^{-1}\left[\frac{\eta}{10}\right]^{-1}\left[\frac{f}{400\ \text{Hz}}\right]^{11/3}\ . \tag{53}$$

The servo frequency probably will have to be significantly lower than the observing frequency, for any tuned detector. This is so that phase noise in the controlling oscillator does not impose excess noise on the position of the signal recycling mirror. Use of a notch in the filtering of the feedback signal should avoid any such problem, although this will have to be of variable frequency with dynamic tuning.

As long as we do not want to observe above ~ 500 Hz, the control of the signal recycling mirror should not be an insurmountable problem.

V. NUMERICAL RESULTS

We devote this section to present systematically the results of a variety of numerical computations based on the above theory. This will illustrate the powerful performance of dynamic tuning under more realistic conditions than described so far.

In paper I we outlined the statistical theory of signal detection and estimation of signal parameters. It turns out that if we know the shape of the signal and the noise is Gaussian the optimal procedure consists of passing the data through a bank of linear filters. The Fourier transform of the other filter is the Fourier transform of the expected signal divided by spectral density of noise. We proved that in the case of a chirp signal we need to pass the data through two banks of filters depending on two parameters: time of arrival t_i and chirp mass $\mathcal{M}$. Then maximize a certain functional formed out of the two filters against the two parameters. The phase and amplitude parameters can then be calculated explicitly. We

have given formulas for the signal-to-noise ratio and the covariance matrix giving the accuracy in the determination of the parameters. Those formulas apply to the case of dynamic tuning within the quasistationary approximation presented in Sec. II.

A. Detector's sensitivity with dynamic tuning

It is very interesting to make a plot of the *sensitivity* of the antenna to a chirp of gravitational radiation. In order to maintain the same criteria we used in previous publications (see, e.g., [5,17]), where we defined sensitivity as $1/S_n(f)$, $S_h(f)$ being the spectral density of noise in the interferometer which appears in the general formula

$$(S/N)^2=2\int_0^\infty \frac{|\tilde{h}(f)|^2}{S_h(f)}df \ , \tag{54}$$

with $|\tilde{h}(f)|^2 \propto f^{-7/3}$ in the present case, we shall here take

$$\text{Sensitivity (dynamic tuning)} \propto \frac{2\pi\tau B - NA^2}{B^2}|\mathcal{I}_s|^2 \tag{55}$$

according to formula (28). Such plot is displayed in Fig. 2, where several cases are differentiated. They correspond to a *perfectly* tuned antenna over the whole frequency range, and to several *mismatched* chirp trackings. The latter are exemplified by $\{\Delta t_i=10$ ms, $\Delta\mathcal{M}=0\}$, $\{\Delta t_i=0$, $\Delta\mathcal{M}=0.01\ \mathcal{M}_{1.4\odot}\}$, and $\{\Delta t_i=10$ ms, $\Delta\mathcal{M}=0.01\ \mathcal{M}_{1.4\odot}\}$, respectively. The latter values are somewhat arbitrary, but still roughly typical of a realistic situation. The figure also shows the sensitivity function for a static configuration of 6 Hz bandwidth, the optimum for this case, cf. Ref. [5]: it is the sharply peaked curve on the far left of the graph. Bandwidth of 6 Hz is also the constant value we have adopted throughout the dynamic tuning. Note how, in all cases, sensitivity improves over a large frequency range thanks to dynamic tuning, even if errors in initial parameter estimation are allowed for. It tends to drop at high frequencies due to the failure of the system to catch up with the large frequency sweep rate occurring at those frequencies.

TABLE I. Values of signal-to-noise ratio (S/N), error in timing (Δt_i), and in mass parameter ($\Delta\mathcal{M}$), and 1D-timing error, i.e., the error in this parameter when all the rest are known, for static broadband standard recycling and for dynamic tuning. Values for the latter correspond to *ideal* dynamic tuning (perfectly tracked chirp) and are given in milliseconds for times and as millimultiples of the mass parameter $\mathcal{M}_{1.4\odot}$ of a binary consisting of two equal stars having each 1.4 solar masses. The entry "GAIN factors" gives an idea of how do both antenna configurations compare.

	S/N	Δt_i	Δt_i (1D)	$\Delta\mathcal{M}$
Broadband	8	2.23	0.122	1.28
Dynamic	112	0.15	0.017	0.08
GAIN factors	14	15	7	15

We thus see that the net effect of dynamic tuning is to make the detector broadband—for chirps, of course—while keeping narrow-band sensitivities.

Table I summarizes the figures reported on earlier in Secs. II and III. They refer to *ideal* dynamic tuning with a constant bandwidth of 1.6 Hz over a frequency integration range from 100 to 500 Hz. Δt_i is given in milliseconds, and $\Delta\mathcal{M}$ in $10^{-3}\,\mathcal{M}_{1.4\odot}$, where $\mathcal{M}_{1.4\odot}$ is the mass parameter of a binary system consisting of two equal stars of 1.4 solar masses each. The table also includes $\Delta t_i(1D)$, which is the accuracy in the determination of t_i when the other parameters are known. As argued at the end of Sec. III, such accuracy could be achieved with a network of detectors (also [6]).

The meaning of *parameter errors* here needs some clarification, for *ideal* dynamic tuning implicitly assumes there are *no* errors at all in the parameters. The clue to the question lies in the fact that, even if he manages to track the chirp exactly, the experimenter will have no

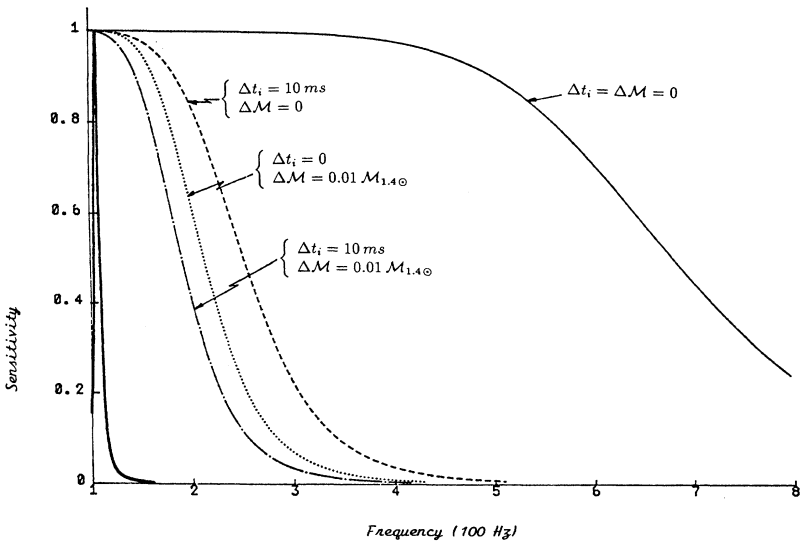

FIG. 2. Sensitivity functions for dynamic tuning. The solid thin line corresponds to perfect tuning, the broken lines to differently mismatched parameters as indicated. On the far left, a plot of static narrow-band dual recycling is also given for comparison. Bandwidth is equal to 6 Hz both for dynamic and static cases. Ordinate units are arbitrary, and frequencies are in 100 Hz.

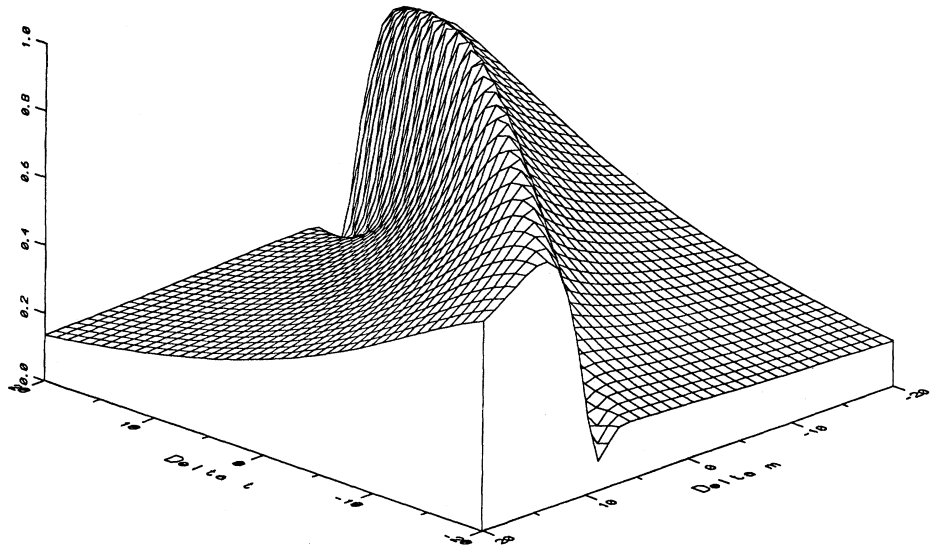

FIG. 3. Perspective plot of the two-dimensional ambiguity function for dynamic tuning. Ordinate units are normalized, so that the highest point on the surface has height 1. In abscissas, Δt is represented in millisecond and $\Delta\mathcal{M}$ in $10^{-3}\,\mathcal{M}_{1.4\odot}$, i.e., thousandths of the mass parameter of a binary system made up to two equal 1.4 solar mass stars.

means of knowing he is doing so with *absolute* certainty—he will only notice his signal-to-noise ratios are very high. So he will still attribute a certain tolerance to the values of t_i and $\mathcal{M}$ he decides on, and it is these tolerances which we give in Table I. They are obtained by use of the two-dimensional *ambiguity function* (cf. paper I), a plot of which is given in Figs. 3 and 4 in the form of a perspective plot and a contour map, respectively.

B. Actual performance of dynamic tuning

As a next step we attempt to calculate what we can achieve by dynamic tuning in practice. We do not know the parameters of the chirp initially; therefore, we propose to keep the detector in the static dual recycling configuration and wait for the chirp. When the chirp arrives we detect it and estimate its parameters *on line* with linear filtering; then we tune the detector with tuning frequency f_T determined by the estimates of the parameters. Of course because of noise there are inevitable errors in our estimates, which are measured by the components of the covariance matrix.

Consequently we have written the following computer program. We calculate the signal-to-noise ratio and covariance matrix for static dual recycling starting from the seismic cutoff frequency of 100 Hz up to a certain frequency f_1. Then in the tuning frequency we insert for the time of arrival t_i the true t_i plus or minus the square root of the C_{tt} component of the covariant matrix (whichever gives the highest tuning offset) and the same

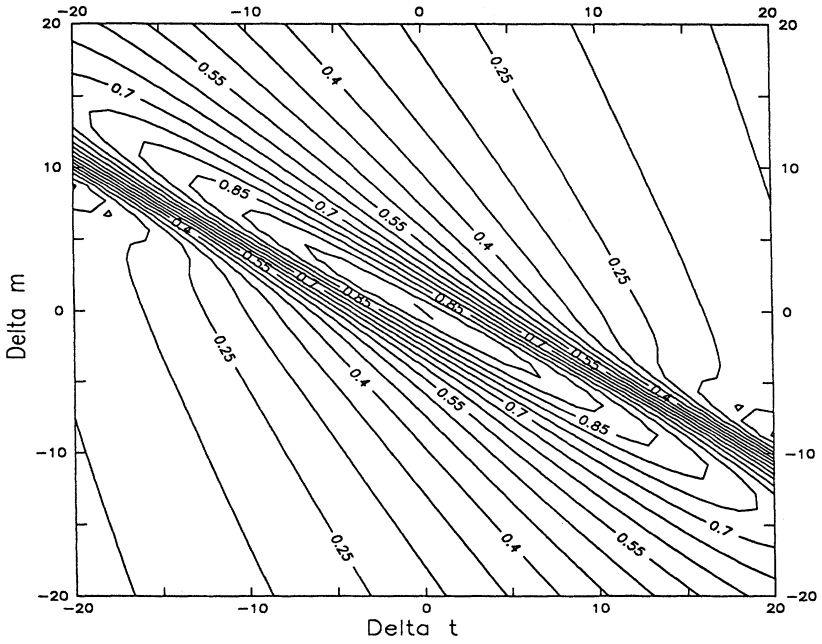

FIG. 4. Contour map for the above surface.

for the chirp mass. This determines the dynamic transfer function. We then calculate the signal-to-noise ratio and covariance matrix for a dynamically tuned detector with the initial frequency f_1 and the final frequency f_b of, say, 500 Hz. The final signal-to-noise ratio is the square root of sum of the squares of the signal-to-noise ratios in the static and dynamic phases. The final covariance matrix Γ is also calculated as the inverse of the Γ matrix formed from the sum of the Γ matrices in the static and dynamic cases. As the frequency f_1 approaches f_s, the initial signal-to-noise ratio is smaller and smaller and consequently the initial accuracy in the determination of parameters is poorer and poorer and the performance of the system is worse and worse. As f_1 approaches f_b, performance tends to that of the static configuration. Therefore we expect that there is an optimum frequency $f_{1_{\text{opt}}}$ that gives highest signal-to-noise ratio and smallest errors in the estimation of parameters.

In Fig. 5 we give a plot of the final S/N and Δt_i for a range of values of the intermediate frequency f_1 corresponding to dynamic tuning with a fixed bandwidth of 6 Hz. The curves confirm the above predictions, but we see that optimum S/N and optimum timing accuracy (i.e., lowest Δt_i) are obtained for slightly different values of f_1. If we take, for example, $f_1=115$ Hz then we find $S/N=39$, $\Delta t_i=0.82$ ms, and $\Delta t_i(1D)=0.12$ ms, always better than corresponding values for static broadband detection (Table I).

We have also considered another sophistication that may have practical implementation. This is to introduce several parameter *updates* during the course of dynamic detection of the chirp. This means making parameter estimations several times during the chirp's life and readjusting tuning parameters at each stage correspondingly (recall the discussion of Sec. IV). We have tested *our* updating strategies; namely, we update every certain equal interval of time, frequency, spectral density and chirp radiated power.

Tables II–V give the results for the above updating strategies with four updates, always for constant bandwidth of 6 Hz, and $f_1=115$ Hz. Inspection of the tables shows that an "evenly spaced spectral density of chirp updating strategy produces the best performance of the four cases considered. This is not a very surprising result, since such spacing in the frequency interval matches the energy distribution (in frequency) of the chirp. The poorest corresponds to equal frequency spacings, not an expected result, either, since giving the same weight to high and low frequencies is clearly a waste.

Note also that the best results (Table IV) differ little from those obtained when parameters are updated at equal intervals of time (Table II). This is good news since it will probably be easiest in practice to part the data for analysis into equal stretches as they happen.

Now, which is the optimum number of updates? A too large number will no doubt be inconvenient because it will benefit poorly from the small amount of information gathered during a short duration sample, due to the considerable computing power required by on-line analysis. A too small number, on the other hand, will miss the opportunity of getting improved accuracies. Take, for example, one single update: S/N is about 39 for this case; *our* updates yield $S/N\sim 65$–a significant improvement–but 15 updates only give $S/N\sim 67$. So the number of 4 here proposed seems to be a balanced tradeoff between the "too many" and the "too few." It is, however, a bit premature to make too detailed assessments of these matters as of now.

Another point to investigate is the bandwidth. So far we have only reported on the results of keeping it *fixed* during the entire process of dynamic tuning, but advantage could be taken from letting it vary as tracking proceeds. We can think for example of a bandwidth increasing with frequency in order to allow for smaller errors in parameter estimation at high frequencies, where the signal-to-noise ratio has already built up to large enough values. One must be very careful, though, not to let the bandwidth grow too much since inequality (12),

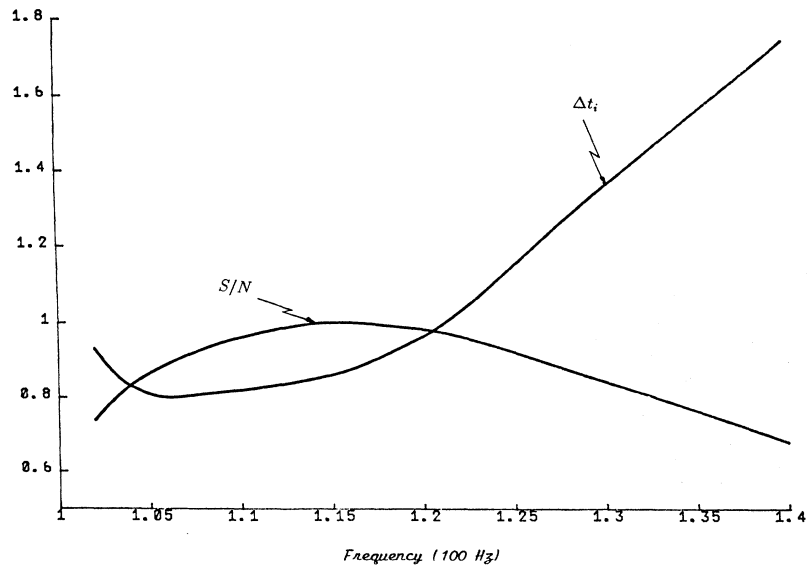

FIG. 5. S/N (convex curve) and Δt_i (concave curve) vs intermediate frequency f_1 (in 100 Hz). Units for the former are normalized so that maximum S/N corresponds to an ordinate unity. Units for Δt_i are in milliseconds.

TABLE II. This table contains the same magnitudes as Table I as entries. They correspond, however, to different antenna settings. Static tuning is assumed during the first stage (from 100 to 115 Hz), then dynamic tuning is switched on with mismatched chirp parameters. These are updated *four* times at equal intervals of *time* as the chirp happens, and the partial results are reported in the table. The last update is completed in the highest frequency, here taken as 500 Hz.

	S/N	Δt_i	$\Delta t_i)(1D)$	$\Delta\mathcal{M}$	
Broadband	7.88	2.23	0.122	1.28	$f_s=100$ Hz
Static	7.9	19.0	3.806	29.08	Up to 115 Hz
Update	26.3	11.9	1.575	14.12	Up to 128 Hz
Update	37.8	4.55	0.456	4.15	Up to 148 Hz
Update	49.6	1.54	0.155	1.11	Up to 189 Hz
Final	64.6	0.39	0.033	0.21	$f_b=500$ Hz
GAIN factors	8.2	5.7	3.7	6.1	

TABLE III. Same as II, except that updates are taken at equal intervals of *frequency* over the integration range.

	S/N	Δt_i	Δt_i $(1D)$	$\Delta\mathcal{M}$	
Broadband	7.88	2.23	0.122	1.28	$f_s=100$ Hz
Static	7.9	19.0	3.806	29.08	Up to 115 Hz
Update	38.1	1.86	0.248	1.38	Up to 211 Hz
Update	48.5	0.78	0.055	0.45	Up to 307 Hz
Update	52.1	0.53	0.038	0.29	Up to 404 Hz
Final	53.3	0.44	0.032	0.24	$f_b=500$ Hz
GAIN factors	6.8	5.0	3.8	5.4	

TABLE IV. Same as Table II, this time for intervals of equal *spectral density* of the chirp.

	S/N	Δt_i	$\Delta t_i(1D)$	$\Delta\mathcal{M}$	
Broadband	7.88	2.23	0.122	1.28	$f_s=100$ Hz
Static	7.9	19.0	3.806	29.08	Up to 115 Hz
Update	27.5	10.9	1.361	12.53	Up to 129 Hz
Update	39.5	3.82	0.383	3.36	Up to 153 Hz
Update	51.4	1.30	0.131	0.90	Up to 200 Hz
Final	64.7	0.40	0.032	0.21	$f_b=500$ Hz
GAIN factors	8.2	5.5	3.8	6.1	

TABLE V. Finally, updates are here taken by intervals where the chirp *radiated power* (i.e., the integral of its spectral density) is equal.

	S/N	Δt_i	$\Delta t_i(1D)$	$\Delta\mathcal{M}$	
Broadband	7.88	2.23	0.122	1.28	$f_s=100$ Hz
Static	7.9	19.0	3.806	29.08	Up to 115 Hz
Update	31.8	7.34	0.787	7.48	Up to 138 Hz
Update	45.3	2.05	0.209	1.58	Up to 175 Hz
Update	56.6	0.80	0.076	0.49	Up to 249 Hz
Final	64.4	0.39	0.031	0.21	$f_b=500$ Hz
GAIN factors	8.2	5.7	3.9	6.1	

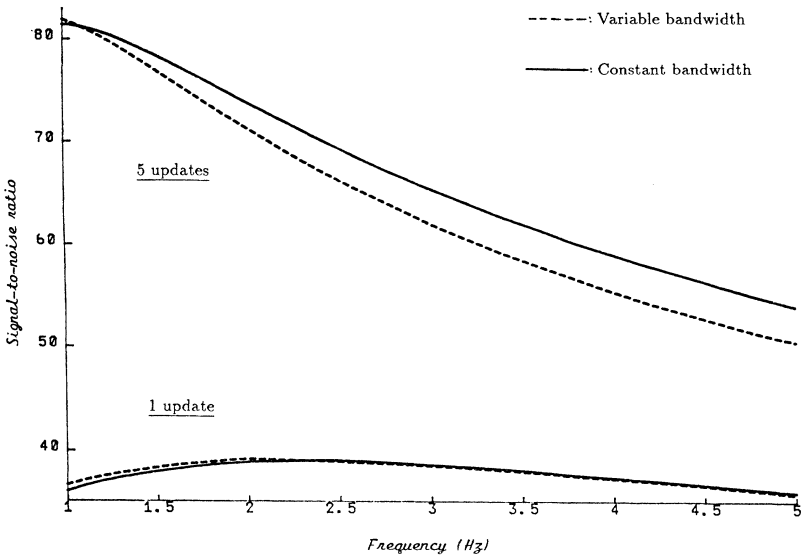

FIG. 6. Signal-to-noise ratios B_0 (in Hz). Solid curves correspond to dynamic tuning with *constant* bandwidth equal to $2B_0$ dashed curves to variable bandwidth [cf. Eq. (56) in the text]. Upper curves derive from a fivefold updating of parameters during dynamic tuning, and lower ones from a single updating (the final). The binary is supposed to be a two 1.4 $\mathcal{M}_\odot$ system 100 Mpc away from the detector.

which lies at the root of our quasistationary approach, must hold all the time.

Next is a sensible choice:

$$B(f)=B_0\left[1+\left[\frac{f}{400\ \text{Hz}}\right]^{8/3}\right], \tag{56}$$

where B_0 is a constant. The formula is *sensible* in the sense that it ensures that (12) holds for a considerable range of frequencies and mass parameters.

In Fig. 6 we give plots of signal-to-noise ratios versus B_0 for a two 1.4 $\mathcal{M}_\odot$ binary. The upper curves correspond to five parameter updates during dynamic tuning, and the lower to just one. Solid curves correspond to a fixed bandwidth (equal to $2B_0$), dashed to variable bandwidth according to (56). The graph shows that parameter updating is a more powerful method to increase sensitivity than to change bandwidth: only for rather short initial bandwidths, causing very poor initial parameter estimation, does the latter result in some improvement over the former.

This should be considered good news, because implementation of a variable bandwidth in the interferometer will require the replacement of the signal recycling mirror by an optical cavity of variable transmission coefficient, a further technical sophistication. A more flexible method than the rather stiff one given by (56), however, should not be excluded *a priori:* any means of improving parameter determination in real time will always be welcome.

VI. CONCLUSIONS

In this paper we propose a new method to operate a laser interferometric gravitational-wave (GW) detector in order to enhance its sensitivity to chirps from coalescing compact binary systems of stars. The method is a variation of narrow-band *dual recycling,* and consists of adjusting the position of the signal recycling mirror M_3 (see Fig. 1) *dynamically,* that is, so that the system is kept in resonance with the *instantaneous* chirp frequency. We have given a formula for the frequency response of the interferometer in such configuration which is the basis for the subsequent analysis, both analytical and numerical.

Although ideally it is seen that enhancement factors in S/N over broadband (static) standard recycling an be as high as 15, it is not sensible to expect them in actual practice: inevitable errors in parameter estimation (necessary for correct tracking) will considerably lower the above limit. So we have assessed in the paper how the initial errors in the estimation of the chirp's parameters affect the detector's performance, i.e., what the final S/N will be and how do initial errors propagate (and eventually improve) during dynamic tuning. The results are that one can realistically expect to reach enhancement factors of about 8 (rather than 15), still a very encouraging prospect.

Dynamic tuning strongly relies on *on-line* data analysis—chirp parameters must obviously be determined as they happen—so enough computing power will be required to quickly pass the data through a bank of filters and make decisions about parameters in *real time.* This needs more powerful computers than are now available, but we still must wait a number of years before GW detector technology is ripe to start implementing dynamic tuning. Progress in computer design over the last two decades, however, has been so important that hopes that requisite machines will be operative in due time do not seem unrealistic.

ACKNOWLEDGMENTS

A. K. acknowledges support from the Polish Science Committee Grant No. KBN 2 1010 91 01. J. A. L. also acknowledges support from the Spanish Ministry of Education, Grant No. PB90-0482-C02-02.

[1] K. S. Thorne, in *300 Years of Gravitation,* edited by S. W. Hawking and W. Israel (Cambridge University Press, Cambridge, England, 1987).
[2] J. P. A. Clark, E. P. J. Van den Heuvel, and W. Sutantyo, Astron. Astrophys. **72**, 120 (1979).
[3] J. Hough *et al.*, GEO proposal, Max-Planck-Institut für Quantenoptik Report No. MPQ 147, 1989 (unpublished).
[4] A. Krolak, J. A. Lobo, and B. J. Meers, Phys. Rev. D **43**, 2470 (1991).
[5] B. F. Schutz, Nature **323**, 310 (1986).
[6] B. F. Schutz (private communication).
[7] R. W. P. Drever, in *Gravitational Radiation,* edited by N. Deruelle and T. Piran (North-Holland, Amsterdam, 1983).
[8] B. J. Meers, Phys. Rev. D **38**, 2317 (1988).
[9] K. A. Strain and B. J. Meers, Phys. Rev. Lett. **66**, 1391 (1991).
[10] A. Krolak, in *Gravitational Wave Data Analysis,* edited by B. F. Schutz (Reidel, Amsterdam, 1989).
[11] B. J. Meers, Phys. Lett. A **142**, 465 (1989).
[12] S. V. Dhurandhar, A. Krolak, B. F. Schutz, and J. Watkins (unpublished).
[13] B. J. Meers and K. A. Strain, Phys. Rev. D **43**, 3117 (1991).
[14] See, e.g., B. J. Meers and K. A. Strain, Phys. Rev. A **44**, 4693 (1991).
[15] B. J. Meers and R. W. P. Drever (unpublished).
[16] A. Krolak, J. A. Lobo, and B. J. Meers (unpublished).
[17] J. A. Lobo, Class. Quantum Grav. **9**, 1385 (1992).
[18] P. Jaranowski and A. Krolak (unpublished).